Tunable Surface-Enhanced Infrared Absorption on Au Nanofilms on Si Fabricated by Self-Assembly and Growth of Colloidal Particles

Sheng-Juan Huo,[†] Qiao-Xia Li,[†] Yan-Gang Yan,[†] Yi Chen,[†] Wen-Bin Cai,*[,†,‡] Qun-Jie Xu,[‡] and Masatoshi Osawa[§]

Shanghai Key Laboratory for Molecular Catalysis and Innovative Materials and Department of Chemistry, Fudan University, Shanghai 200433, China, Department of Environmental Engineering, Shanghai University of Electric Power, Shanghai 200090, China, and Catalysis Research Center, Hokkaido University, Sapporo 001-0021, Japan

Received: May 17, 2005; In Final Form: June 30, 2005

Au colloids were used to fabricate nanoscale-tunable Au nanofilms on silicon for surface-enhanced IR absorption bases in both ambient and electrochemical environments. This wet process incorporates the self-assembly of colloidal Au monolayer using 3-aminopropyl trimethoxysilane as the organic coupler with subsequent chemical plating in an Au(III)/hydroxylamine solution. FTIR spectroscopy in transmission mode of the probe species SCN^- was used to evaluate the apparent surface enhancement in IR absorption of 2D Au colloid arrays and chemically plated Au particles. The nanostructure of Au films was examined by atomic force microscopy. The IR and AFM results show that the apparent surface enhancement factor (1−2 orders of magnitude) increases with increasing sizes and/or contact, and the severe aggregation of Au nanoparticles may cause the bipolar band shape. Cyclic voltammetry on the Au nanofilm obtained by the above nucleation and growth strategy exhibits a feasible electrochemical stability and behavior. In situ ATR-FTIR measurement of *p*-nitrobenzoic acid adsorption demonstrates that the as-grown Au film yields rather promising surface enhancement as well.

Introduction

Surface-enhanced infrared absorption spectroscopy (SEIRAS) has gained a reputation as a sensitive spectroscopic tool for the detection of a variety of adsorbate molecules at both metal−ambient and metal−liquid interfaces.[1−13] It has been widely applied to surface trace analysis, bio-sensing, electrosorption, and electrocatalysis because of its significant amplification of surface signal and simple surface selection rule. The surface-enhanced infrared absorption (SEIRA) can be observed easily on metal island films prepared by vacuum evaporation or sputtering and electrochemical or electroless deposition. Metal colloids also support the enhancement.[7,8a] Like surface-enhanced Raman scattering (SERS), SEIRA is chiefly of electromagnetic origin, that is, due to an increase in the local optical field exciting the adjacent molecules.[2] Metal particles much smaller than the wavelength of light facilitate the interaction of the infrared radiation with the metal and adsorbed molecules, resulting in the enhancement. It has been well established that the enhancement is greatly affected by the size, shape, and proximity of metal particles. Therefore, the fabrication of nanostructured metal films with tunable size, shape, and proximity is of vital importance for probing and utilizing SEIRA effect.

As compared to the intensive study of SERS on specially engineered Au and Ag nanostructures including self-assembled colloidal monolayer,[14] the corresponding issue for SEIRA has received far less attention. Van Duyne and co-workers[15] pioneered in addressing this issue by building surface architectures of 2D Ag particles based on a nanosphere lithography technique for ex situ SEIRA measurements in attenuated-total-reflection (ATR) mode. In their work, ordered arrays of uniformly sized silver nanoparticles with triangular cross-sectional shapes were prepared by vacuum-evaporating an Ag nanofilm on a mask of polystyrene nanosphere monolayer self-assembled onto a Si or Ge substrate followed by removal of the mask. Wieckowski and co-workers[16] used organic couplers to link discrete Pt−Ru nanoparticles onto an Au bulk substrate from a suspension solution of commercially available Pt−Ru electrocatalyst powder. In their external IRAS, measurement on the CO adsorption on that Pt−Ru modified Au electrode showed a unipolar band with an enhancement factor of less than 20.

In this report, we propose a wet-chemistry strategy for fabricating Au nanofilms on IR transparent Si with controlled particle sizes and spatial distribution. This strategy is based on an initial two-dimensional immobilization of a discrete Au colloid array on an aminosilane-modified Si with subsequent growth of Au nuclei by self-catalyzed electroless deposition.

The advantage of this strategy for preparing SEIRA-active films over the existing dry and wet processes is 2-fold. First, the most frequently used dry processes including vacuum evaporation and sputtering possess the disadvantages of high cost, poor adhesion, and band distortion. To overcome these problems, wet processes, mainly chemical and electrochemical deposition, have been introduced very recently for preparing coinage metals and Pt group metals on IR transparent substrates.[12,13] However, the electrochemical deposition is applicable only to conducting substrates. The chemical deposition technique is free from this requirement, but seeding of Pd nuclei before the deposition of the desired metal is usually necessary. In

* Corresponding author. Phone: +86-21-55664050. Fax: +86-21-65641740. E-mail: wbcai@fudan.edu.cn.
[†] Fudan University.
[‡] Shanghai University of Electric Power.
[§] Hokkaido University.

10.1021/jp052585v CCC: $30.25
Published on Web 08/02/2005

SCHEME 1: Protocol for Assembling and Growing Au Colloidal Nanoparticle Layer on a Hydroxylized Si Substrate

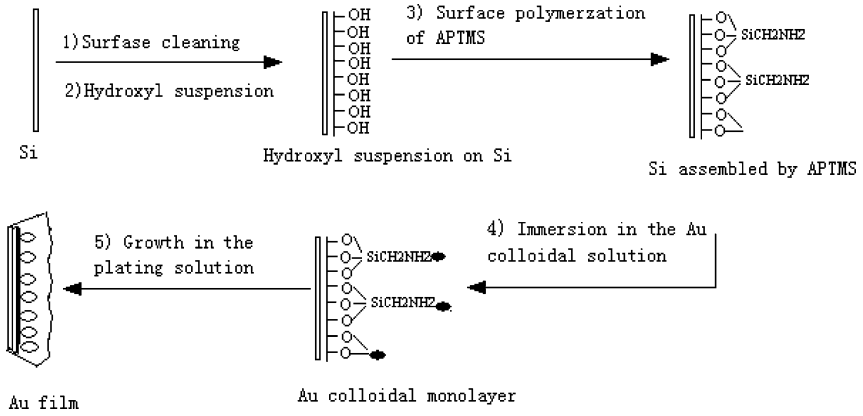

addition, the pretreatment of the substrate surface with HF damages the substrate. Our current work is partly motivated along this line by examining an alternate wet process for preparing SEIRA-active substrates applicable to SEIRAS measurements in both ambient and electrochemical environments. As compared to previous chemical deposition of conducting Au and Pt nanofilm on Si reported,[13a−e] the current protocol is totally Pd^{2+} and F^- free, thus greatly reducing possible contamination of unwanted trace metals co-deposited and damage to ATR elements.

Second, surfaces built from colloidal Au particles have a tunable 2D nanoscaled roughness defined solely by the particle diameter. The synthesis of monodisperse Au colloids with desired particle sizes is quite mature because of the contribution from Natan's group.[22] Moreover, as compared to a suspension of commercial metallic powder, a colloidal solution provides a much more reliable and stable source for depositing a monolayer of nanoparticles on surface. Furthermore, the growth of Au nanoparticle nuclei via surface-catalyzed reduction of Au^{3+} by hydroxylamine can be used to increase the particle size and coverage.[22] The nucleation and growth of colloidal Au particles will allow for a better control of surface nanoarchitecture. Similar tactics was used for surface plasmon resonance spectroscopy on Au colloidal films on glass substrate,[18] and for UV−vis spectroscopy on Au and Ag colloidal films on quartz substrate.[19]

For SEIRA spectroscopy in transmission and ATR modes, IR transparent substrates should be used for supporting metallic colloids. Ag colloids being spread on an IR transparent KRS-5 plate by drop-coating and Au colloids being filtrated onto porous polyethylene membranes were reported as SEIRA-active substrates for transmission measurement.[7,8a] Nevertheless, those methods did not provide any control of surface roughness and aggregation, and consequently poor reproducibility in SEIRA effect can be expected. Furthermore, they are not suitable for electrochemical SEIRA measurement due to the lack of conductivity. To our best knowledge, this strategy of self-assembly and seeding growth has not been adapted for the fabrication of metallic nanofilms on IR transparent Si for ambient and electrochemical SEIRA studies.

Experimental Section

Chemicals. (3-Aminopropyl)-trimethoxysilane (APTMS) was obtained from Aldrich. Gold chloride, hydrocycammonlum chloride (or hydroxylamine hydrochloride), sodium borohydride, sodium hydroxide, tri-sodium citrate, paranitrobenzoic acid (PNBA), sulfuric acid, hydrogen peroxide (30% v/v), hydrochloric acid (37% v/v), ammonia solution (28% v/v), and acetone were obtained from Shanghai Chemical Reagent Corp. All chemicals were of analytical grade. All aqueous solutions were made using ultrapure water from a Milli-Q system (Millipore).

Preparation of Colloidal Particles. Three Au colloidal solutions with different sizes were prepared according to the recipes and procedures of Dong et al. (Sol A),[18] Frens (Sol B),[23] and Natan et al. (Sol C).[22] Briefly for Sol A, 1 mL of 1%(w/v) aqueous $HAuCl_4$ was added to 100 mL of ultrapure H_2O under vigorous stirring followed by the addition of 1 mL of 1% (w/v) aqueous sodium citrate within 1 min. After an additional 1 min, 1 mL of 0.075% (w/v) $NaBH_4$ in 1% sodium citrate was added. The solution was stirred for 5 min and then stored at 4 °C. For Sol B, 1% gold chloride was diluted by 100 mL of ultrapure water, followed by adding 3.5 mL of 1% sodium citrate in refluxing condition under vigorous stirring for 20 min. For Sol C, to a stirred solution of boiling 100 mL of 0.01% $HAuCl_4$, seed Au colloids (ca. 2.5-nm-diameter) were added coincidentally with the addition of 38.8 mM sodium citrate (final concentration 0.17 mM). This mixture was boiled for 15 min and stirred for an additional 10 min while cooling.

Substrate Preparation. A 1 cm × 1 cm cut n-type Si wafer (10 Ω·cm, 0.3 mm thick, Shanghai) or a Si hemicylinder prism (nondoped, PASTEC, Osaka) with a 2 cm × 2.5 cm basal plane was cleaned by sonicating in acetone and water in turn. The silicon was then immersed into a solution of H_2O_2:NH_4OH:H_2O (1:1:5) and H_2O_2:HCl:H_2O (1:1:5) (90 °C) for 10 min to remove possible contaminants. Hydroxyl suspension on Si surfaces was then performed according to one of the following two pretreatments: (1) the Si wafer was annealed in a muffle under 700 °C for 20 min followed by 5 min immersion a piranha solution (3:1 H_2SO_4:30%H_2O_2) at 80 °C; or (2) the Si prism was immersed in a boiling piranha solution for 20 min (***Caution:*** *Piranha solution is a powerful oxidizing reagent and reacts violently with organic compounds. It should be handled with extreme care*). Afterward, the Si sample was rinsed thoroughly with Milli-Q water, and the working surface was immersed in a solution of APTMS (5% aqueous solution) for 6 h and rinsed with copious amounts of water upon removal. The aminosilanized Si surface was subsequently immersed in Sols A, B, or C for up to 12 h for assembling a monolayer of Au nanoparticles. In particular, the Si surface assembled with 2.5-nm colloidal Au array was immersed in a 4-mL mixed solution containing 0.5% $HAuCl_4$ and 0.04% hydrocycammonlum chloride for chemical plating Au at room temperature. The growth of the Au nanoparticles was controlled by the electroless plating times. Scheme 1 represents the procedure for embedding

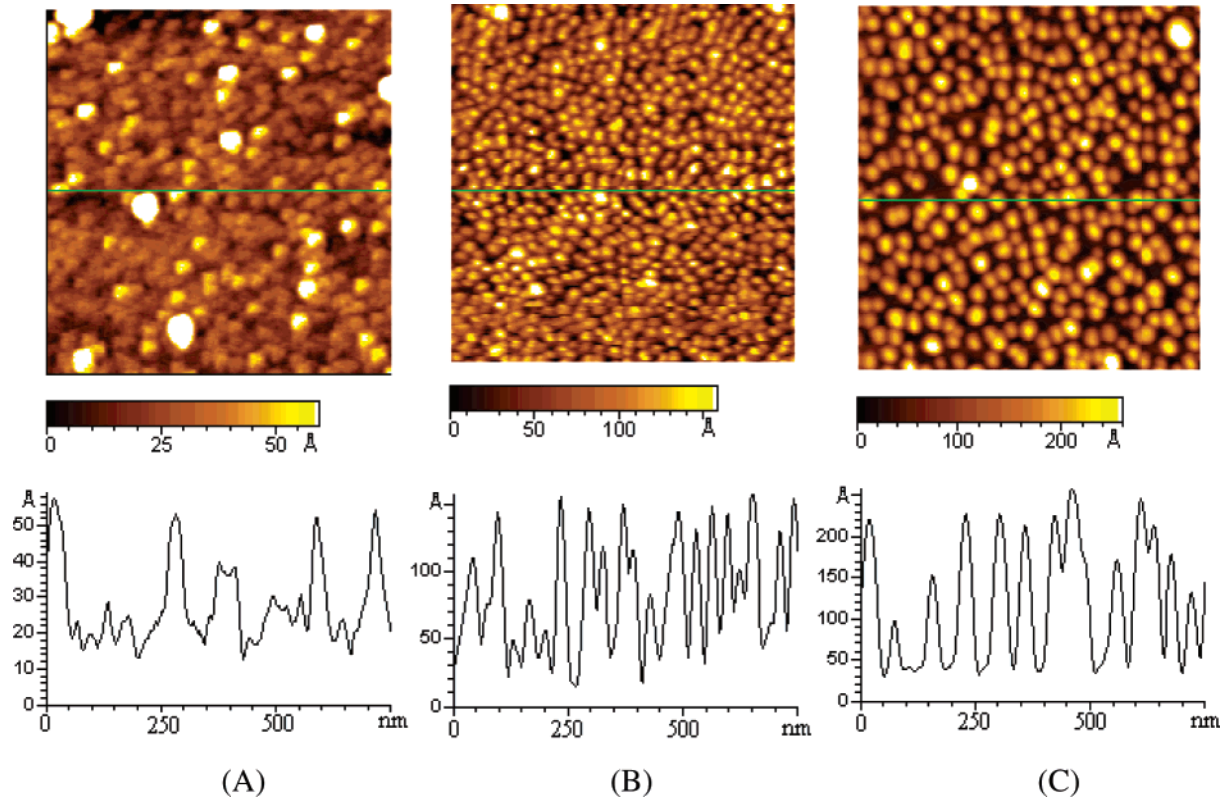

Figure 1. AFM images (750 nm × 750 nm) of 2D 2.5-nm (A), 12-nm (B), and 23-nm (C) Au colloidal particles assembled on aminosilanized Si substrates.

an array of Au colloidal particles and their subsequent electroless deposition.

SEIRA Spectroscopy, Electrochemistry, and AFM. A Nicolet Magna-IR 760 FT-IR spectrometer equipped with a liquid nitrogen cooled HgCdTe (MCT) detector was used for SEIRAS measurements and was operated at a resolution of 4 cm^{-1}. Spectra of the Au nanofilm/electrolyte interfaces were acquired with the so-called Kretschmann attenuate-total-reflection (ATR) configuration (prism/thin metal film/solution geometry) with an incident angle of 70°, the details of which can be found elsewhere.[2,9a] The transmission mode was used for acquiring spectra of SCN^- adsorption on Au nanoparticle-immobilized Si surfaces. An aliquot of 0.01 M KSCN in acetone solution was dispersed onto Si surfaces to achieve a mass of 500 ng cm^{-2} for Au colloid-coated Si and that of 5 μg cm^{-2} for bare Si without Au. The spectra were recorded after the solvent was evaporated in air.

A CHI 630B electrochemistry workstation (CH Instruments, Shanghai) was employed for potential/current control and to record the cyclic voltammograms. All electrode potentials are cited with a reversible hydrogen electrode (RHE), unless specifically addressed.

Atomic force microscopy (AFM) images were acquired with tapping mode under ambient conditions with a Pico-SPM (Molecular Imaging, Tempe, AZ). Si cantilevers with a spring constant between 1.2 and 5.5 N m^{-1} were used at resonance frequencies between 60 and 90 kHz.

Results and Discussion

Transmission SEIRA on Au Colloid Arrays. Natan's group established a relationship between the surface plasmon band of colloidal Au solution and the particle sizes.[22b] The monodispersed Au colloids of Sol A, Sol B, and Sol C produced strong surface plasmon bands at 513, 518, and 524 nm in UV−vis absorption spectra (not shown), corresponding to an average diameter of ca. 2.5, 12, and 23 nm, respectively.[18a,22b] The Au colloid solutions with pH 6 are dominantly negatively charged due to the adsorption of anions, while the amino groups are mainly positively charged. The positively charged functional group NH_2 of self-assembled aminosilane interacts strongly with negatively charged Au colloidal particles, acting as an excellent organic coupler between Au nanoparticle monolayers and hydroxylized Si surfaces. Figure 1 shows the AFM images of 2D self-assembled Au particle arrays with colloid sizes of 2.5 nm (A), 12 nm (B), and 23 nm (C). Well-dispersed metal particles are identified. The heights of the feature are in reasonable agreement with the particle sizes deduced from UV−vis measurement. Nevertheless, the size of the particles does not agree with that of the Au colloids used. This is due to the well-known convolution of the AFM tip with the true particle size.[24] As a result, the individual particles of the 2.5-nm colloid cannot be clearly differentiated, and the images of 12- and 23-nm colloidal particles are significantly magnified with respect to their real sizes. It was reported that 12-nm Au nanoparticles on Si exhibit a size of 28 nm in AFM images.[23b] Nevertheless, the 2D nanoparticle array is confirmed by AFM images for the 12- and 23-nm diameter Au colloids, and nanoparticles can be seen in Figure 1C that are larger than those in Figure 1B. Further examination of these images reveals that the particles are closed-spaced but physically isolated in two dimensions (with an average interparticle spacing around the particle's diameter) as a result of a balance of interparticle electrostatic repulsion and the high affinity of particle-amine group. All of these immobilized Au nanofilms are in stark contrast to those obtained by evaporating Au onto an organic coupler modified substrate, where a 3-nm thick Au layer was sufficient to be continuous and conductive.[25] This again demonstrates that the above wet chemistry process is favorable for controlling discrete spheroidal

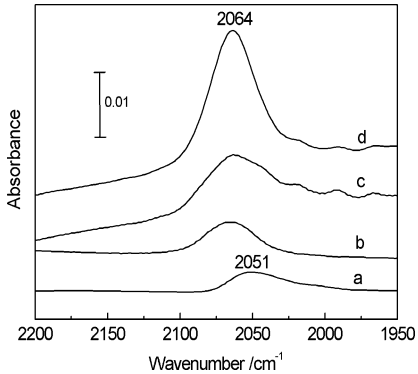

Figure 2. IR transmission spectra of KSCN dispersed on bare Si and 2D colloidal Au-coated Si: 5 μg cm^{-2} of KSCN on bare Si substrate (curve a); 500 ng cm^{-2} of KSCN on 2.5-nm (curve b), 12-nm (curve c), and 23-nm (curve d) Au colloid arrays-coated Si.

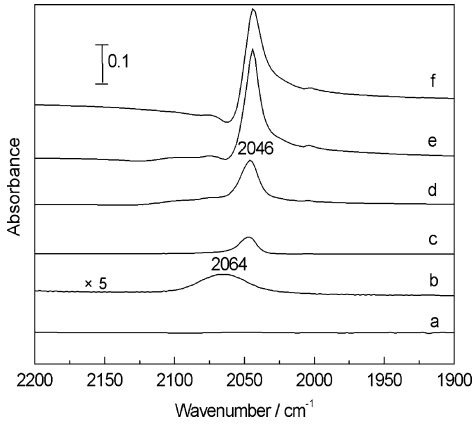

Figure 3. Transmission spectra of 500 ng cm^{-2} KSCN dispersed on bare Si substrate (a), and Si initially coated with 2.5-nm Au colloid followed by reduction growth in a mixed 0.5% $HAuCl_4$ and 0.04% hydrocycammonlum chloride for 0 (b, 5-fold magnified), 1.5 (c), 3.5 (d), 5.5 (e), and 7.5 min (f), respectively.

island nanostructures, providing a unique template for studying the size- and spacing-dependent SEIRA effect.

The SEIRA effect of three self-assembled Au nanoparticle films was examined by comparing the intensity and shape of the ν_{CN} band of SCN^- adsorbed by drop-coating an acetone solution of KSCN onto each sample. Figure 2 illustrates IR transmission spectra for 500 ng cm^{-2} of KSCN dispersed on the Au films on Si prepared from Au colloids with diameters of 2.5 (curve b)-, 12 (curve c)-, and 23 (curve d)-nm on Si. A spectrum for 5 μg cm^{-2} of KSCN coated on bare Si (curve a) is also shown in the figure for comparison. The KSCN deposited on the bare Si shows the ν(CN) vibration at 2051 cm^{-1} as is observed in the transmission measurement using KBr pellets,[26,27a] while the corresponding mode on the Au immobilized Si surfaces locates at 2064 cm^{-1}. The shift of the ν_{CN} band position indicates that the signal mainly comes from interfacial SCN^- on Au. Three adsorption geometries are possible for SCN^- on Au, that is, via the N end, S end, or bridge-bonding.[27b] It is well established that the latter two configurations yield significant blue shifts of the ν_{CN} band, usually going higher than 2100 cm^{-1}. The observed small shift is suggestive of the preferential adsorption of SCN via the end N on Au. Most notable in this figure is that the intensity of the ν_{CN} band increases with increasing particle size. The apparent surface enhancement factors were roughly estimated to be 15, 35, and 62 by simple comparison of integrated ν_{CN} band intensities obtained with and without Au colloid arrays on Si after calibrating KSCN loadings.

The effect of the particle size on the enhanced ν_{CN} band for the adsorbed SCN^-on colloidal Au arrays can be explained by the SEIRA mechanism[2] as follows. When a colloidal Au film is illuminated with IR radiation, collective electron oscillations (plasmons) are excited in the nanoparticles and a strong electric field is produced around the Au surfaces.[2] The enhanced electric field excites vibrations of SCN^- species in the near vicinity of the surface. Because of the dipole coupling between the electron oscillations of Au colloids and molecular vibrations of SCN^-, optical properties of the Au nanoparticles are modulated. The modulation is significant at frequencies of the ν_{CN} vibration, so it can be detected through the change in absorbance or reflectance of the metal film. The stronger absorption of the larger particles may result from the stronger surface plasmon resonance as well as the stronger dipole coupling.

Transmission SEIRA on Au Films Grown on 2D Nanoparticle Arrays. Surface nanostructures such as particle size and aggregation state of Pt group metal nanofilms are known to affect significantly the band intensity and shape of SEIRA spectra. One primary motivation of our work is to explore tuning SEIRA effect by a seeding growth process in which aqueous Au(III) was chemically deposited onto 2.5-nm-diameter Au nuclei on Si. Figure 3 shows the transmission spectra of 500 ng cm^{-2} loading of KSCN on a bare Si (curve a), a 2.5-nm-diameter colloidal Au array (curve b), and Au thin films chemically grown on colloidal Au arrays in a mixed Au(III) and hydroxylamine solution for different times (curves c−f). Three important features can be found in Figure 3. First, the peak position of the ν_{CN} band is red-shifted from 2064 cm^{-1} for the 2D Au colloidal array to around 2046 cm^{-1} by the postdeposition of Au. The difference in the band shift may reflect the difference in crystalline orientations and surface potentials that existed for Au nanoparticles before and after chemical plating.[27]

Second, the IR bands become remarkably narrower, as compared to those shown in Figure 2. One probable explanation is that the originally immobilized Au colloids have various crystalline orientations and defects; after chemical plating, certain crystalline orientations on colloidal seeds may preferentially grow, contributing to narrower bandwidth and different band position.

Third, the band intensity and band shape depend on the plating time. Apparent enhancement factors are estimated to be 54, 204, 352, and 374 for the plating times of 1.5, 3.5, 5.5, and 7.5 min, respectively. As the plating time reaches 7.5 min, bipolar band shape appears in the transmission measurement. The corresponding AFM images are shown in Figure 4a−d, it can be seen that at the early stage of the chemical plating, the growth of nuclei array seems not linearly due to slightly different initial particle sizes in a 2D array, leaving many "dark voids" among the particle islands (or larger interparticle spacing) as shown in Figure 4a. With increasing time, these "dark voids" became small and less (see Figure 4b). Upon further growth, the particles contact physically and form a rather coherent gold layer (see Figure 4c). Nevertheless, severe particle aggregation can be seen in Figure 4d, when the deposition time extends further.

In other words, with this protocol, the nanoparticle sizes, interparticle spacing, and even the aggregation state can be easily tuned. The increased band intensity and the final emergence of bipolar band shape with deposition time are closely related to increased particle size and decreased proximity, and the aggregation of nanoparticles in Au nanofilm as the chemical plating proceeds. A similar tendency was observed by Griffith and co-workers in their study of SEIRA of CO on platinized Pt

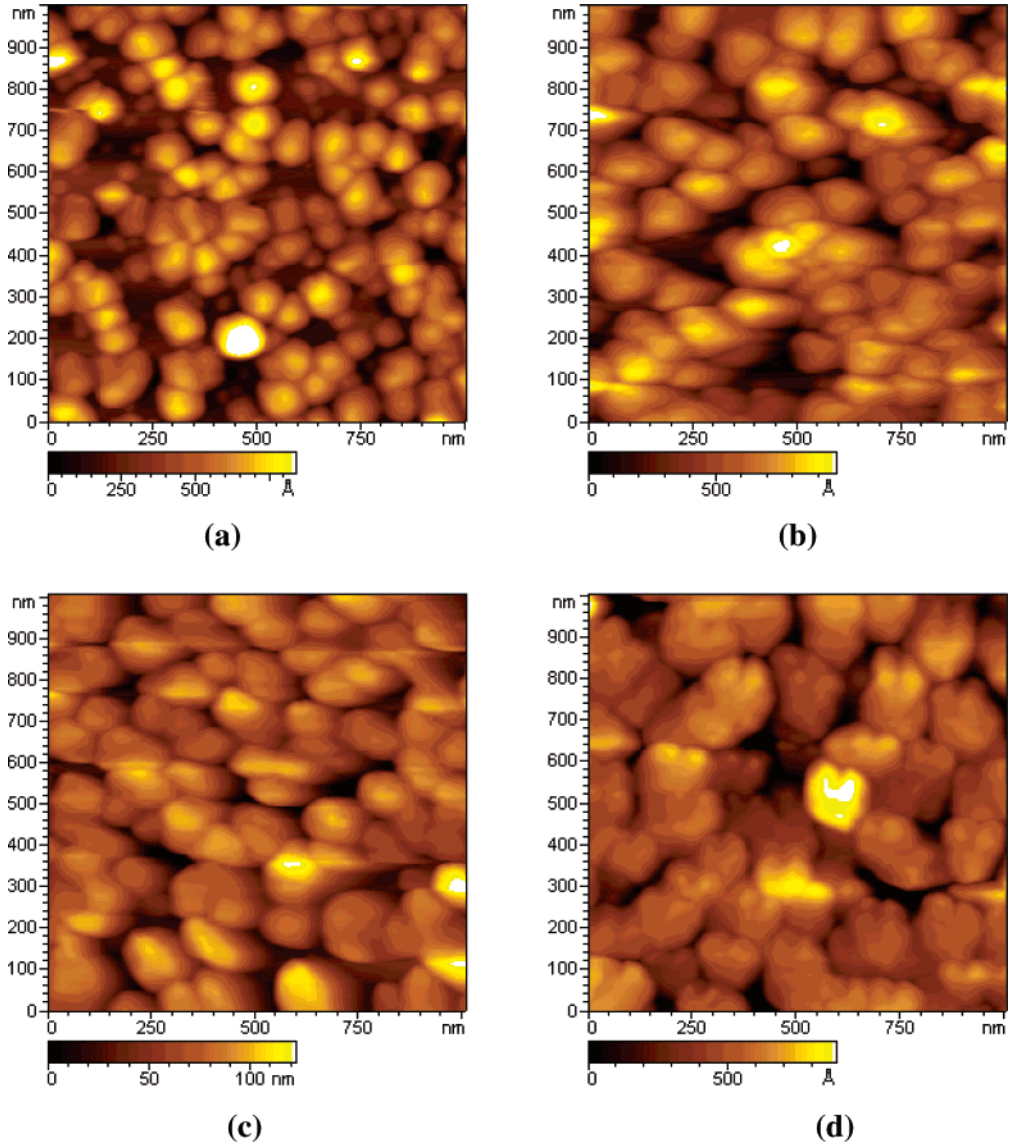

Figure 4. AFM images of immobilized 2.5-nm-diamter Au colloid array on Si wafer after chemical plating for different times: (a) 1.5 min, (b) 3.5 min, (c) 5.5 min, and (d) 7.5 min.

surfaces.[4b] By using Bergman representation of effective dielectric function for simulation, they successfully elucidated the observed intensity and band shape change with the degree of platinization on Pt.

Electrochemical ATR-SEIRA of an As-Grown Au Nanofilm. The strategy of initial self-assembly of Au nuclei and subsequent chemical plating can also be extended to fabricate ATR-SEIRA active Au electrodes. In comparison to previous chemical deposition of Au nanofilms on the basal plane of an ATR Si prism,[13a−e] this unique wet process does not require corrosive and reactive F^- toward Si and Pd nuclei layers for the deposition to proceed, thus preventing the co-deposition of unwanted metals and the corrosion attack on the costly ATR-Si prism. By using Au colloids as the nuclei and the mild reducing agent of hydroxylamine, ATR-SEIRA active Au nanofilm electrode can be successfully fabricated without the above-mentioned problems.

Two chief concerns in electrochemical ATR-SEIRA application are the adhesion and the signal enhancement of thus-obtained Au nanofilms. In the literature report, Au nanofilms prepared by the dry process on bare Si usually have poor adhesion. Adhesion can be improved with an organic coupler, but the SEIRA effect loses.[6,25] By contrast, the Au nanofilms on Si prepared by the current strategy possess improved adhesion and strong enhancement. Complete adhesion was retained after the Au films were subject to immersion in common organic solvents (such as acetone, methanol) or aqueous acid (such as 0.1 M $HClO_4$, 0.1 M H_2SO_4) or salt

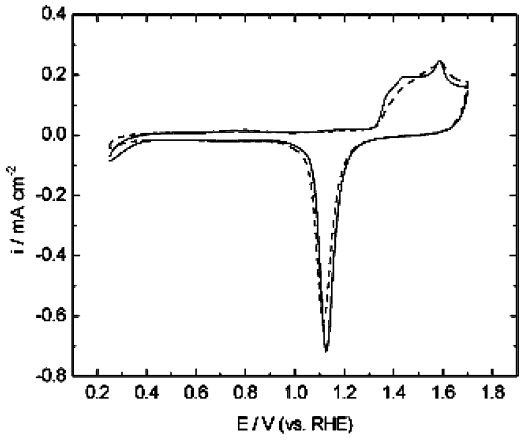

Figure 5. Cyclic voltammograms for an as-deposited Au nanofilm electrode in 0.1 M $HClO_4$ at 50 mV s^{-1}: - - - -, 1st scan; —, 50th scan.

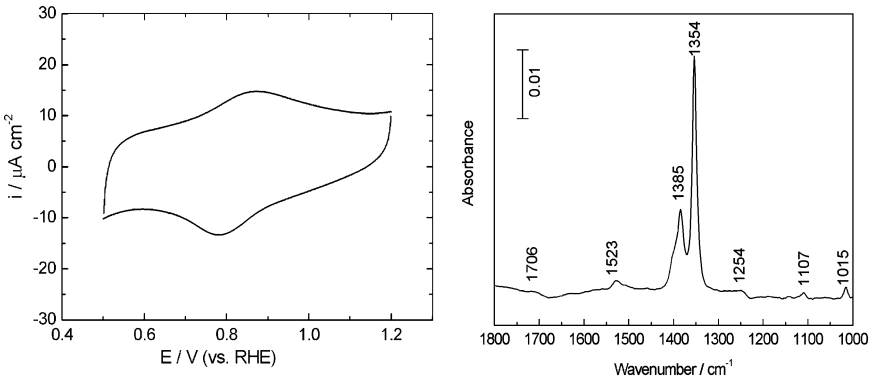

Figure 6. (a) Cyclic voltammogram of reversibly absorbed PNBA at an as-deposited Au nanofilm electrode in 0.1 M $HClO_4$; (b) ATR-SEIRA spectrum measured at 1.0 V for the Au nanofilm electrode in the same solution, reference spectrum was collected at 0.5 V.

solutions (such as 0.1 M $NaClO_4$) for 1 day. Most importantly, they are suitable for electrochemical measurement. Figure 5 presents cyclic voltammograms of the 1st and 50th cycles for an as-deposited Au nanofilm electrode on the reflective plane of an ATR-Si prism in 0.1 M $HClO_4$ between 0.25 and 1.70 V at 50 mV s^{-1}. It can be seen the cyclic voltammetric response is the same as that of a bulk Au electrode. From the reduction charge of Au oxide, a roughness factor of 2.5 can be estimated by taking 0.44 mC cm^{-2} for an ideally smooth Au surface.[17a] The Au film upon increasing potential scan exhibits a somewhat preferred crystalline orientation and slightly increased surface roughness. No peeling of the Au deposit from the substrate was found even after 2 h of continuous cycling.

To examine the in situ ATR-SEIRA of thus-obtained Au nanofilm, the PNBA molecule was selected as the probe. Figure 6a shows the cyclic voltammogram recorded for an as-grown Au nanofilm electrode in 1 mM PNBA + 0.1 M $HClO_4$ in the potential region of 0.50−1.20 V at a scan rate of 50 mV s^{-1}. A couple of peaks at around 0.80 V were ascribed to the adsorption and desorption of PNBA on Au electrode. Figure 6b is the corresponding ATR-FTIR spectrum acquired at 1.0 V. The reference potential was 0.50 V. The strong bands at 1354 and 1385 cm^{-1} are assigned to the symmetric stretching modes of nitro and carboxylate groups, that is, $\nu_{s(ONO)}$ and $\nu_{s(OCO)}$, respectively.[28] The weak bands at 1015, 1107, and 1523 cm^{-1} are assigned to symmetric ring modes ν_{10}, ν_9, and antisymmetric NO_2 stretching $\nu_{as(ONO)}$, respectively.[28] The bands (1706 and 1254 cm^{-1}) characterizing carboxylic group can hardly be seen, suggestive of *p*-nitrobenzoate species bound to the Au surface through the carboxylate oxygen atoms with a bridging coordination. This spectral feature is in agreement with literature report, and the intensities of the two strong bands are comparable to those obtained for the Au nanofilms on ATR Si prepared by other tactics.[13a,28b] The peak intensity of the $\nu_{s(ONO)}$ mode at 1354 cm^{-1} is 0.035 Abs for unpolarized IR radiation, that is, 150-fold as strong as that obtained on a mechanically polished Au electrode with IRAS measurement.[28c]

Conclusion

Fabrication of nanostructured metal films with well-tuned size, shape, and proximity is of vital importance for probing and utilizing SEIRA effect. We have demonstrated a wet process to fabricate nanoscale-tunable Au nanofilms on Si for both ambient and electrochemical SEIRA spectroscopy, by self-assembling two-dimensional arrays of colloidal Au particles onto immobilized polymers having pendant NH_2 groups followed by the seeding growth of the Au nuclei. The polymers are formed by condensation of functionalized alkoxysilanes onto hydroxylized Si surface. FTIR spectroscopy in transmission mode of the probe species SCN^- was used to evaluate the apparent surface enhancement in IR absorption on 2D Au colloid arrays and chemically plated Au nanoparticle films. AFM was used to characterize the nanostructure of Au films. The results show that the apparent surface enhancement factor (1−2 orders of magnitude) increases as the Au nanoparticle size increases and the interparticle spacing decreases, and the severe aggregation of nanoparticles may cause the bipolar band shape. Cyclic voltammetry on the Au nanofilm obtained by the above nucleation and growth strategy exhibits a good electrochemical stability and response. In situ ATR-FTIR measurement of *para*-nitrobenzoic acid adsorption demonstrates that the as-grown Au film yields rather promising surface IR absorption enhancement as well.

Current tactics require no F^- and Pd for growing metallic nanofilms on Si, reducing greatly the possible co-deposition of a trace amount of unwanted metals and the corrosive attack on ATR Si prisms. Our recent test shows that the overall time for preparing SEIRA-active Au nanofilm electrode may be significantly shortened; further investigation of optimizing the preparation conditions is underway and will be reported in due course. It is expected that the above strategy can be a useful alternate wet process for preparing SEIRA-tunable Au nanofilms for ex situ and in situ applications.

Acknowledgment. The NSFC (Nos. 20333040, 20473025), the SRFDP (No. 20040246008), the NCET and the SNPC (No. 0452nm064-2), China (W.-B.C.), and the MEXT (No. 14205121 and Priority Areas 417), Japan (M.O.), are gratefully acknowledged for financial support.

References and Notes

(1) Hartstein, A.; Kirtley, J. R.; Tsang, J. C. *Phys. Rev. Lett.* **1980**, *45*, 201.

(2) (a) Osawa, M. In *Handbook of Vibrational Spectroscopy*; Chalmers, J. M., Griffiths, P. R., Eds.; John Wiley & Sons: Chichester, U.K., 2002; Vol. 1, pp 785−799. (b) Osawa, M. *Bull. Chem. Soc. Jpn.* **1997**, *70*, 2861.

(3) Wandlowski, T.; Ataka, K.; Pronkin, S.; Diesing, D. *Electrochim. Acta* **2004**, *49*, 1233.

(4) (a) Bjerke, A. E.; Griffiths, P. R. *Appl. Spectrosc.* **2002**, *56*, 1275. (b) Bjerke, A. E.; Griffiths, P. R.; Theiss, W. *Anal. Chem.* **1999**, *71*, 1967.

(5) Zhang, Z.; Imae, T. *Langmuir* **2001**, *17*, 4564.

(6) Goutev, N.; Futamata, M. *Appl. Spectrosc.* **2003**, *57*, 506−513.

(7) Kang, S. Y.; Jeon, C.; Kim, K. *Appl. Spectrosc.* **1998**, *52*, 278.

(8) (a) Seelenbinder, J. A.; Brown, C. W.; Pivarnik, P.; Rand, A. G. *Anal. Chem.* **1999**, *71*, 1963. (b) Seelenbinder, J. A.; Brown, C. W.; Urish, D. W. *Appl. Spectrosc.* **2000**, *54*, 367.

(9) (a) Cai, W.-B.; Wan, L.-J.; Noda, H.; Hibino, Y.; Ataka, K.; Osawa, M. *Langmiur* **1998**, *14*, 6992. (b) Cai, W.-B.; Amano, M.; Osawa, M. *J. Electroanal. Chem.* **2001**, *500*, 147.

(10) Loster, M.; Friedrich, K. A. *Surf. Sci.* **2003**, *523*, 287.

(11) (a) Yajima, T.; Uchida, H.; Watanabe, M. *J. Phys. Chem. B* **2004**, *108*, 2654. (b) Watanabe, M.; Zhu, Y. M.; Uchida, H. *J. Phys. Chem. B* **2000**, *104*, 1762. (c) Zhu, Y. M.; Uchida, H.; Watanabe, M. *Langmuir* **1999**, *15*, 875.

(12) Yan, Y.-G.; Li, Q.-X.; Huo, S.-J.; Ma, M.; Cai, W.-B.; Osawa, M. *J. Phys. Chem. B* **2005**, *109*, 7900.

(13) (a) Miyake, H.; Ye, S.; Osawa, M. *Electrochem. Commun.* **2002**, *4*, 973. (b) Miyake, H.; Osawa, M. *Chem. Lett.* **2004**, *33*, 278. (c) Miki, A.; Ye, S.; Osawa, M. *Chem. Commun.* **2003**, 1500. (d) Chen, Y. X.; Miki, A.; Ye, S.; Sakai, H.; Osawa, M. *J. Am. Chem. Soc.* **2003**, *125*, 3680. (e) Miki, A.; Ye, S.; Senzaki, T.; Osawa, M. *J. Electroanal. Chem.* **2004**, *563*, 23. (f) Rodes, A.; Orts, J. M.; Pérez, J. M.; Feliu, J. M.; Aldaz, A. *Electrochem. Commun.* **2003**, *5*, 56.

(14) (a) Zhu, Z. H.; Zhu, T.; Liu, Z. F. *Nanotechnology* **2004**, *15*, 357. (b) Tian, Z. Q.; Ren, B.; Wu, D. Y. *J. Phys. Chem. B* **2002**, *106*, 9463. (c) Dick, L. A.; McFarland, A. D.; Haynes, C. L.; Van Duyne, R. P. *J. Phys. Chem. B* **2002**, *106*, 853. (d) Gunnarsson, L.; Bjerneld, E. J.; Xu, H.; Petronis, S.; Kasemo, B.; Kall, M. *Appl. Phys. Lett.* **2001**, *78*, 802. (e) Grabar, K. G.; Freeman, R. G.; Hommer, M. B.; Natan, M. J. *Anal. Chem.* **1995**, *67*, 735. (f) Chumanov, G.; Sokolov, K.; Gregory, B. W.; Cotton, T. M. *J. Phys. Chem. B* **1995**, *99*, 9466. (g) Freeman, R. G.; Grabar, K. C.; Allison, K. J.; Bright, R. M.; Davis, J. A.; Guthrie, A. P.; Hommer, M. B.; Jackson, M. A.; Smith, P. C.; Walter, D. G.; Natan, M. J. *Science* **1995**, *267*, 1629.

(15) Jensen, T. R.; Van Duyne, R. P.; Johnson, S. A.; Maroni, V. A. *Appl. Spectrosc.* **2000**, *54*, 371.

(16) Park, S.; Wiekowski, A.; Weaver, M. J. *J. Am. Chem. Soc.* **2003**, *125*, 2282.

(17) (a) Sun, S.-G.; Cai, W.-B.; Wan, L.-J.; Osawa, M. *J. Phys. Chem. B* **1999**, *103*, 2460. (b) Chen, W.; Sun, S.-G.; Zhou, Z. Y.; Chen, S.-P. *J. Phys. Chem. B* **2003**, *107*, 9808. (c) Sun, S.-G. In *Catalysis and Electrocatalysis at Nanoparticle Surfaces*; Wieckowski, A., Savinova, E. R., Vayenas, C. G., Eds.; Marcel Dekker: New York, 2003; Chapter 21.

(18) (a) Jin, Y. D.; Kang, X. F.; Song, Y. H.; Zhang, B. L.; Cheng, G. J.; Dong, S. J. *Anal. Chem.* **2001**, *73*, 2843. (b) Cheng, W. L.; Dong, S. J.; Wang, E. K. *J. Phys. Chem. B* **2004**, *108*, 19146.

(19) Frederix, F.; Friedt, J. M.; Choi, K. H.; Laureyn, W.; Campitelli, A.; Mondelaers, D.; Maes, G.; Borghs, G. *Anal. Chem.* **2003**, *75*, 6894.

(20) (a) Bright, R. M.; Musick, M. D.; Natan, M. J. *Langmuir* **1998**, *14*, 5695. (b) Lyon, L. A.; Pena, D. J.; Natan, M. J. *J. Phys. Chem. B* **1999**, *130*, 5826.

(21) Sagara, T.; Kato, N.; Nakashima, N. *J. Phys. Chem. B* **2002**, *106*, 1205.

(22) (a) Brown, K. R.; Natan, M. J. *Langmuir* **1998**, *14*, 726. (b) Brown, K. R.; Walter, D. G.; Natan, M. J. *Chem. Mater.* **2000**, *12*, 306.

(23) Frens, G. *Nat. Phys. Sci.* **1972**, *241*, 20.

(24) (a) Grabar, K. G.; Brown, K. R.; Keating, C. D.; Stranick, S. J.; Tang, S. L.; Natan, M. J. *Anal. Chem.* **1997**, *69*, 471. (b) Zheng, J. W.; Zhu, Z. H.; Chen, H. F.; Liu, Z. F. *Langmuir* **2000**, *16*, 4409.

(25) Dunaway, D. J.; McCarley, R. L. *Langmuir* **1994**, *10*, 3598.

(26) Nakamoto, K. *Infrared and Raman Spectra of Inorganic and Coordination Compounds, Part A, Theory and Applications in Inorganic Chemistry*, 5th ed.; John Wiley & Sons: New York, 1997.

(27) (a) Li, X.; Gewirth, A. A. *J. Am. Chem. Soc.* **2003**, *125*, 11674. (b) Pecile, C. *Inorg. Chem.* **1966**, *5*, 210. (c) Bailey, R. A.; Kozak, S. L.; Michelson, T. W. *Coord. Chem. Rev.* **1971**, *6*, 407. (d) Tian, Z. Q.; Ren, B.; Mao, B. W. *J. Phys. Chem. B* **1997**, *101*, 1338

(28) (a) Ernsterbunner, E. E.; Girling, R. B.; Hester, R. E. *J. Chem. Soc., Faraday Trans.* **1978**, *74*, 1540. (b) Noda, H.; Wan, L.-J.; Osawa, M. *Phys. Chem. Chem. Phys.* **2001**, *3*, 3336. (c) Xiao, X.-Y.; Sun, S.-G.; *Electrochim. Acta* **2000**, *45*, 2897. (d) Merklin, G. T.; Griffiths, P. R. *J. Phys. Chem. B* **1997**, *101*, 5810.